

Charmless Hadronic B Decays to Exclusive Final States with a K^* , ρ , ω , or ϕ Meson.

CLEO Collaboration

(September 12, 2018)

Abstract

We present results of searches for B -meson decays to charmless final states that include a K^* , ρ , ω , or ϕ meson accompanied by a second meson. Using the entire data sample of 9.7×10^6 $B\bar{B}$ pairs collected with the CLEO II and CLEO II.V detectors, we observe a signal for the decay $B^+ \rightarrow \omega\pi^+$, and measure a branching fraction of $\mathcal{B}(B^+ \rightarrow \omega\pi^+) = (11.3_{-2.9}^{+3.3} \pm 1.5) \times 10^{-6}$. We also see evidence for the decay $B^0 \rightarrow \omega K^0$, and set limits for the decays $B^0 \rightarrow \rho^0\pi^0$ and $B^0 \rightarrow K^{*0}\pi^0$. In addition to these new results, we also summarize previous CLEO results on related channels. All quoted results are preliminary.

M. Bishai,¹ S. Chen,¹ J. Fast,¹ J. W. Hinson,¹ J. Lee,¹ N. Menon,¹ D. H. Miller,¹
 E. I. Shibata,¹ I. P. J. Shipsey,¹ Y. Kwon,^{2,*} A.L. Lyon,² E. H. Thorndike,² C. P. Jessop,³
 K. Lingel,³ H. Marsiske,³ M. L. Perl,³ V. Savinov,³ D. Ugolini,³ X. Zhou,³ T. E. Coan,⁴
 V. Fadeyev,⁴ I. Korolkov,⁴ Y. Maravin,⁴ I. Narsky,⁴ R. Stroynowski,⁴ J. Ye,⁴ T. Wlodek,⁴
 M. Artuso,⁵ R. Ayad,⁵ E. Dambasuren,⁵ S. Kopp,⁵ G. Majumder,⁵ G. C. Moneti,⁵
 R. Mountain,⁵ S. Schuh,⁵ T. Skwarnicki,⁵ S. Stone,⁵ A. Titov,⁵ G. Viehhauser,⁵
 J.C. Wang,⁵ A. Wolf,⁵ J. Wu,⁵ S. E. Csorna,⁶ K. W. McLean,⁶ S. Marka,⁶ Z. Xu,⁶
 R. Godang,⁷ K. Kinoshita,^{7,†} I. C. Lai,⁷ P. Pomianowski,⁷ S. Schrenk,⁷ G. Bonvicini,⁸
 D. Cinabro,⁸ R. Greene,⁸ L. P. Perera,⁸ G. J. Zhou,⁸ S. Chan,⁹ G. Eigen,⁹ E. Lipeles,⁹
 M. Schmidtler,⁹ A. Shapiro,⁹ W. M. Sun,⁹ J. Urheim,⁹ A. J. Weinstein,⁹ F. Würthwein,⁹
 D. E. Jaffe,¹⁰ G. Masek,¹⁰ H. P. Paar,¹⁰ E. M. Potter,¹⁰ S. Prell,¹⁰ V. Sharma,¹⁰
 D. M. Asner,¹¹ A. Eppich,¹¹ J. Gronberg,¹¹ T. S. Hill,¹¹ D. J. Lange,¹¹ R. J. Morrison,¹¹
 T. K. Nelson,¹¹ J. D. Richman,¹¹ R. A. Briere,¹² B. H. Behrens,¹³ W. T. Ford,¹³
 A. Gritsan,¹³ H. Krieg,¹³ J. Roy,¹³ J. G. Smith,¹³ J. P. Alexander,¹⁴ R. Baker,¹⁴
 C. Bebek,¹⁴ B. E. Berger,¹⁴ K. Berkelman,¹⁴ F. Blanc,¹⁴ V. Boisvert,¹⁴ D. G. Cassel,¹⁴
 M. Dickson,¹⁴ P. S. Drell,¹⁴ K. M. Ecklund,¹⁴ R. Ehrlich,¹⁴ A. D. Foland,¹⁴ P. Gaidarev,¹⁴
 L. Gibbons,¹⁴ B. Gittelman,¹⁴ S. W. Gray,¹⁴ D. L. Hartill,¹⁴ B. K. Heltsley,¹⁴
 P. I. Hopman,¹⁴ C. D. Jones,¹⁴ D. L. Kreinick,¹⁴ T. Lee,¹⁴ Y. Liu,¹⁴ T. O. Meyer,¹⁴
 N. B. Mistry,¹⁴ C. R. Ng,¹⁴ E. Nordberg,¹⁴ J. R. Patterson,¹⁴ D. Peterson,¹⁴ D. Riley,¹⁴
 J. G. Thayer,¹⁴ P. G. Thies,¹⁴ B. Valant-Spaight,¹⁴ A. Warburton,¹⁴ P. Avery,¹⁵
 M. Lohner,¹⁵ C. Prescott,¹⁵ A. I. Rubiera,¹⁵ J. Yelton,¹⁵ J. Zheng,¹⁵ G. Brandenburg,¹⁶
 A. Ershov,¹⁶ Y. S. Gao,¹⁶ D. Y.-J. Kim,¹⁶ R. Wilson,¹⁶ T. E. Browder,¹⁷ Y. Li,¹⁷
 J. L. Rodriguez,¹⁷ H. Yamamoto,¹⁷ T. Bergfeld,¹⁸ B. I. Eisenstein,¹⁸ J. Ernst,¹⁸
 G. E. Gladding,¹⁸ G. D. Gollin,¹⁸ R. M. Hans,¹⁸ E. Johnson,¹⁸ I. Karliner,¹⁸ M. A. Marsh,¹⁸
 M. Palmer,¹⁸ C. Plager,¹⁸ C. Sedlack,¹⁸ M. Selen,¹⁸ J. J. Thaler,¹⁸ J. Williams,¹⁸
 K. W. Edwards,¹⁹ R. Janicek,²⁰ P. M. Patel,²⁰ A. J. Sadoff,²¹ R. Ammar,²² P. Baringer,²²
 A. Bean,²² D. Besson,²² R. Davis,²² S. Kotov,²² I. Kravchenko,²² N. Kwak,²² X. Zhao,²²
 S. Anderson,²³ V. V. Frolov,²³ Y. Kubota,²³ S. J. Lee,²³ R. Mahapatra,²³ J. J. O'Neill,²³
 R. Poling,²³ T. Riehle,²³ A. Smith,²³ S. Ahmed,²⁴ M. S. Alam,²⁴ S. B. Athar,²⁴ L. Jian,²⁴
 L. Ling,²⁴ A. H. Mahmood,^{24,‡} M. Saleem,²⁴ S. Timm,²⁴ F. Wappler,²⁴ A. Anastassov,²⁵
 J. E. Duboscq,²⁵ K. K. Gan,²⁵ C. Gwon,²⁵ T. Hart,²⁵ K. Honscheid,²⁵ H. Kagan,²⁵
 R. Kass,²⁵ J. Lorenc,²⁵ H. Schwarthoff,²⁵ E. von Toerne,²⁵ M. M. Zoeller,²⁵ S. J. Richichi,²⁶
 H. Severini,²⁶ P. Skubic,²⁶ and A. Undrus²⁶

¹Purdue University, West Lafayette, Indiana 47907

²University of Rochester, Rochester, New York 14627

³Stanford Linear Accelerator Center, Stanford University, Stanford, California 94309

⁴Southern Methodist University, Dallas, Texas 75275

*Permanent address: Yonsei University, Seoul 120-749, Korea.

†Permanent address: University of Cincinnati, Cincinnati OH 45221

‡Permanent address: University of Texas - Pan American, Edinburg TX 78539.

- ⁵Syracuse University, Syracuse, New York 13244
- ⁶Vanderbilt University, Nashville, Tennessee 37235
- ⁷Virginia Polytechnic Institute and State University, Blacksburg, Virginia 24061
- ⁸Wayne State University, Detroit, Michigan 48202
- ⁹California Institute of Technology, Pasadena, California 91125
- ¹⁰University of California, San Diego, La Jolla, California 92093
- ¹¹University of California, Santa Barbara, California 93106
- ¹²Carnegie Mellon University, Pittsburgh, Pennsylvania 15213
- ¹³University of Colorado, Boulder, Colorado 80309-0390
- ¹⁴Cornell University, Ithaca, New York 14853
- ¹⁵University of Florida, Gainesville, Florida 32611
- ¹⁶Harvard University, Cambridge, Massachusetts 02138
- ¹⁷University of Hawaii at Manoa, Honolulu, Hawaii 96822
- ¹⁸University of Illinois, Urbana-Champaign, Illinois 61801
- ¹⁹Carleton University, Ottawa, Ontario, Canada K1S 5B6
and the Institute of Particle Physics, Canada
- ²⁰McGill University, Montréal, Québec, Canada H3A 2T8
and the Institute of Particle Physics, Canada
- ²¹Ithaca College, Ithaca, New York 14850
- ²²University of Kansas, Lawrence, Kansas 66045
- ²³University of Minnesota, Minneapolis, Minnesota 55455
- ²⁴State University of New York at Albany, Albany, New York 12222
- ²⁵Ohio State University, Columbus, Ohio 43210
- ²⁶University of Oklahoma, Norman, Oklahoma 73019

I. INTRODUCTION

The study of charmless hadronic decays of B mesons plays a key role in understanding the phenomenon of CP violation within the Standard Model [1]. Large asymmetries are predicted for some exclusive final states, and although the relatively small branching fractions of $\mathcal{O}(10^{-5})$ currently limit the experimental reach for such studies, the sensitivity of the CLEO II detector allows us to measure branching fractions for some decay modes. B factory experiments that just started or are about to begin operation should expand this already rich field of investigation.

Theoretical predictions typically make use of effective Hamiltonians, often with factorization assumptions [2–11]. The strong interaction between particles in the final state complicates these predictions. However, experimental measurements can be used to verify the validity of the assumptions made, to tune the parameters of the theory in order to make further predictions, and to understand the relative importance of the various decay amplitudes that contribute to a particular decay. Recently, it has been suggested [12–14] that published experimental results on charmless hadronic B decays indicate that $\cos\gamma < 0$, where γ is one of the angles of the unitarity triangle. This somewhat disagrees with current fits to the information most sensitive to CKM matrix elements [16]. Again, more experimental results can help clarify the situation.

In this paper, we present preliminary results of searches for B -meson decays to exclusive two-body final states [15] that include a K^* , ρ , ω , or ϕ meson, and another low-mass meson. We concentrate on new results, although previously reported results are included for completeness.

II. DATA SAMPLE AND INITIAL EVENT SELECTION

The data were collected with the CLEO II [17] and CLEO II.V [18] detectors at the Cornell Electron Storage Ring (CESR). For most of the new results the data sample includes all data collected prior to the de-commissioning of CLEO II.V, in preparation for a significant upgrade. The total integrated luminosity is 9.13 fb^{-1} for the reaction $e^+e^- \rightarrow \Upsilon(4S) \rightarrow B\bar{B}$, which corresponds to 9.7×10^6 $B\bar{B}$ pairs. This is between 40% and a factor of three more statistics than for previously published results [19,20]. In addition, we re-analyzed the CLEO II data set with improved calibration constants and track-fitting procedure, allowing us to extend our geometric acceptance and track quality requirements. This has led to an overall increase in reconstruction efficiency of 10–20 % compared to the previously published analyses. For studies of background from continuum processes, we also collected 4.35 fb^{-1} of data at a center-of-mass energy below the threshold for $B\bar{B}$ production.

The final states of the decays under study are reconstructed by combining detected photons and charged pions and kaons. The resonances in the final state are identified via the decay modes $\rho \rightarrow \pi\pi$, $K^* \rightarrow K\pi$, $\omega \rightarrow \pi^+\pi^-\pi^0$, and $\phi \rightarrow K^+K^-$. The detector elements most important for the analyses presented here are the tracking system, which consists of several individual concentric detectors operating inside a 1.5 T superconducting solenoid, and the high-resolution electromagnetic calorimeter, made of 7800 CsI(Tl) crystals. For CLEO II, the tracking system consists of a 6-layer straw tube chamber, a 10-layer precision

drift chamber, and a 51-layer main drift chamber. The main drift chamber also provides a measurement of the specific ionization loss, used for particle identification. For CLEO II.V the 6-layer straw tube chamber was replaced by a 3-layer double-sided-silicon vertex detector, and the gas in the main drift chamber was changed from an argon-ethane to a helium-propane mixture.

Reconstructed charged tracks are required to pass quality cuts based on their track fit residuals and impact parameter in both the r - ϕ and r - z planes, and on the number of main drift chamber measurements. Each event must have a total of at least four good charged tracks. The specific ionization (dE/dx) measured in the drift layers is used to distinguish kaons from pions. Expressed as the number of standard deviations from the expected value, S_i ($i = \pi$ or K), it is required to satisfy $|S_i| < 3.0$. Electrons are rejected based on dE/dx and the ratio of the measured track momentum and the associated shower energy in the calorimeter. Muons are rejected by requiring that charged tracks penetrate fewer than seven interaction lengths of material. Pairs of charged tracks used to reconstruct K^0 s (via $K_S^0 \rightarrow \pi^+\pi^-$) are required to have a common vertex displaced from the primary interaction point. The invariant mass of the two charged pions is required to be within two standard deviations (10 MeV) of the nominal K_S^0 mass. Furthermore, the K_S^0 momentum vector, obtained with a mass-constrained kinematic fit of the charged pions' momenta, is required to point back to the beam spot.

Photons are defined as isolated showers, not matched to any charged tracks, with a lateral shape consistent with that of photons, and with a measured energy of at least 30 (50) MeV in the calorimeter region $|\cos\theta| < 0.71$ (≥ 0.71), where θ is the polar angle. Pairs of photons are used to reconstruct π^0 s. The momentum of the pair is obtained with a kinematic fit of the photons' momenta with the π^0 mass constrained to its nominal value. The resolution of the invariant mass of the two photons depends on the momentum of the π^0 and is between 5 and 10 MeV/ c^2 . We require the reconstructed mass to be within 3σ on the low side of the nominal π^0 mass, and 2σ on the high side.

III. ANALYSIS TECHNIQUE

The primary means of identification of B meson candidates is through their measured mass and energy. The quantity ΔE is defined as $\Delta E \equiv E_1 + E_2 - E_b$, where E_1 and E_2 are the energies of the two mesons in the final state, and E_b is the beam energy. The beam-constrained mass of the candidate is defined as $M \equiv \sqrt{E_b^2 - |\mathbf{p}|^2}$, where \mathbf{p} is the measured momentum of the candidate. We use the beam energy instead of the measured energy of the B candidate to improve the mass resolution by about one order of magnitude.

The large background from continuum quark-anti-quark ($q\bar{q}$) production can be reduced with event shape cuts. Because B mesons are produced almost at rest, the decay products of the $B\bar{B}$ pair tend to be isotropically distributed, while particles from $q\bar{q}$ production have a more jet-like distribution. The cosine of the angle θ_S between the sphericity axis [21] of the charged particles and photons forming the candidate B and the sphericity axis of the remainder of the event should have a flat distribution for B mesons and be strongly peaked at ± 1.0 for continuum background. We require $|\cos\theta_S| < 0.8$. For final states containing an ω or ϕ meson we use the thrust [22] axis instead of the sphericity, and we

require $|\cos\theta_T| < 0.9$. We also form a Fisher discriminant (\mathcal{F}) [23] with the momentum scalar sum of charged particles and photons in nine cones of increasing polar angle around the sphericity axis of the candidate, the angle of the sphericity axis of the candidate with respect to the beam axis, and $R_2 = H_2/H_0$, the ratio of the second and zeroth Fox-Wolfram moments [24]. For analyses with an ω or ϕ in the final state, the thrust axis replaces the sphericity axis, and the angle between the candidate's momentum vector and the beam axis replaces R_2 .

The specific final states investigated are identified via the reconstructed invariant masses of the B daughter resonances. For vector-pseudoscalar final states, further separation of signal events from combinatoric background is obtained through the use of the defined angular helicity state of the vector meson in the final state. The observable \mathcal{H} is the cosine of the angle between the direction of the B meson and the vector meson daughter decay direction (normal to the decay plane for the ω), both in the vector meson's rest frame.

Signal event yields for each mode are obtained with unbinned, multi-variable maximum likelihood (ML) fits. We also perform event counting analyses that apply tight constraints on all variables described above. Results for the latter are consistent with the ones presented below. For each input event, the likelihood (\mathcal{L}_i) is defined as

$$\mathcal{L}_i = \sum_{i=1}^m n_i \mathcal{P}_i$$

where \mathcal{P}_i are the probabilities for each of the m hypotheses of the fit, and n_i , the free parameters of the fit, are the number of events in the overall sample for each hypothesis. The \mathcal{P}_i are the product of the probability distribution functions (PDFs) for each of the fit's input variables. For N input events, the overall likelihood is then

$$\mathcal{L} = \frac{e^{-(\sum n_i)} N!}{N!} \prod_{i=1}^N \mathcal{L}_i,$$

where the first term takes into account the Poisson fluctuations in the number of events. In all cases, the fit includes hypotheses for signal decay modes and the dominant continuum background. For a few channels indicated below, we also include a hypothesis for background from other B decay modes. For all others, we verified that this component is negligible.

The variables used in the fit are ΔE , M , \mathcal{F} , resonance masses, and \mathcal{H} as appropriate. For pairs of final states differentiated only by the identity (charged pion or kaon) of one of the two mesons, we also use the dE/dx measurement, S_i , for the high-momentum track and fit for both modes simultaneously. Correlations between input variables were investigated and found to be negligible. For each decay mode investigated, the signal PDFs for the input variables are determined with fits to high-statistics Monte Carlo event samples generated with a GEANT [25] based simulation of the CLEO detector response. The parameters of the background PDFs are determined with similar fits to the sum of off-resonance data and a sideband region of on-resonance data in ΔE and M . For M , the sideband is defined by $5.2 < M < 5.3$ GeV/ c^2 . For ΔE the sideband varies depending on the decay mode; details are given in the sections below. Sideband regions for each of the other input variables are also included in the likelihood fit sample.

IV. RESULTS

Table I gives all the measurement results. Details specific to various final states are given in separate sections below. Results for decay modes with a ϕ meson in the final state and of the types $\rho^0 h^+$ and $K^{*0} h^+$, where h^+ is a charged pion or kaon, are based on a data sample of 5.8×10^6 $B\bar{B}$ pairs. Results for final states $\rho^- h^+$, $K^{*+} h^-$, and $\rho^0 K^0$ are based on a sample of 7.0×10^6 $B\bar{B}$ pairs. Shown in the table are the signal event yield, the efficiency, the product of the efficiency and the relevant branching fractions of particles in the final state, the statistical significance of the observed yield in standard deviations, the branching fraction central value with statistical and systematic error, and the corresponding 90% confidence level upper limit. The one standard deviation statistical error on the central value is determined by finding the values where the quantity $\chi^2 = -2 \ln(\mathcal{L}/\mathcal{L}_{\max})$ changes by one unit, where \mathcal{L}_{\max} is the point of maximum likelihood.

Systematic errors are separated into two major components. The first is systematic errors in the PDFs, which are determined with variations of the PDF parameters within their uncertainty, taking into account correlations between parameters. The second component is systematic errors associated with event selection and efficiency factors. These are determined with studies of independent data samples. For branching fraction central values, the systematic error is the quadrature sum of the two components. For upper limits, the likelihood function is integrated to find the yield value that corresponds to 90% of the total area. This value is then increased by its systematic error, and the efficiency is reduced by one standard deviation of its systematic error when calculating the final upper limit.

Table II shows the final results for each decay mode investigated. The third column of the table indicates whether the result is from this work or from an earlier analysis. For observations the final result is reported as a branching fraction central value, while for modes where the yield is not sufficiently significant we quote the 90% confidence level upper limit. Also in the table are previously published theoretical estimates.

A. Final states including an ω meson.

The results for decay modes including an ω meson in the final state were obtained with the full data sample (9.7×10^6 $B\bar{B}$ pairs). The final selection prior to the likelihood fit requires $|\Delta E| < 200$ MeV. In Table I, the final state ωh^+ represents the sum of the ωK^+ and $\omega \pi^+$ states ($h^+ \equiv K^+$ or π^+). For ωK^* and $\omega \rho$ final states, the resonance mass sidebands are $830 < M_{K^*} < 950$ MeV/ c^2 and $600 < M_\rho < 950$ MeV/ c^2 , respectively, and cross-feeds between those decay modes are ignored when performing the fit. For $K^{*0} \rightarrow K^+ \pi^-$, there are two possible assignments for the K^+ . The choice is made based on the dE/dx information of the tracks. For $\rho^0 \rightarrow \pi^+ \pi^-$ the two charged tracks are simply assumed to be pions.

The maximum likelihood fit for ωK^{*0} and $\omega \rho^0$ includes a hypothesis for background from generic B decays. PDFs for this hypothesis are obtained from a sample of Monte Carlo generated events that corresponds to approximately 1.7 times the size of the on-resonance data sample. The yield for $\omega \rho^0$ is entirely consistent with cross-feed from ωK^{*0} . The quoted branching fraction central value has been adjusted to take this into account. For the final states ωK^{*+} and $\omega \rho^+$, the π^0 from K^{*+} or ρ^+ decay defines the daughter direction. Since the

TABLE I. Measurement results. Columns list the final states with resonance decay modes as subscripts, event yield from the fit, reconstruction efficiency ϵ , total efficiency including secondary branching fractions \mathcal{B}_s , statistical significance (σ), branching fraction central value \mathcal{B} , and the corresponding 90% confidence level upper limit. For central values the first error is statistical and the second systematic.

Final state	Yield(events)	ϵ (%)	$\epsilon\mathcal{B}_s$ (%)	Signif.	$\mathcal{B}(10^{-6})$	90% UL(10^{-6})
$\omega\pi^+$	$28.5^{+8.2}_{-7.3}$	29	26	6.2	$11.3^{+3.3}_{-2.9} \pm 1.5$	17
$\omega\pi^0$	$1.5^{+3.5}_{-1.5}$	22	19	0.6	$0.8^{+1.9}_{-0.8} \pm 0.5$	5.8
ωK^+	$7.9^{+6.0}_{-4.7}$	29	26	2.1	$3.2^{+2.4}_{-1.9} \pm 0.8$	8.0
ωK^0	$7.0^{+3.8}_{-2.9}$	24	7.4	3.9	$10.0^{+5.4}_{-4.2} \pm 1.5$	21
ωh^+	$35.6^{+8.9}_{-8.0}$	29	26	7.3	$14.3^{+3.6}_{-3.2} \pm 2.1$	21
$\omega\rho^+$	$10.8^{+6.6}_{-5.3}$	7.1	6.3	2.8	$18^{+11}_{-9} \pm 6$	47
$\omega\rho^0$	$3.7^{+6.0}_{-3.7}$	18	16	0.9	$0.0^{+5.7}_{-0.0} \pm 2.9$	11
ωK^{*+}	$1.0^{+3.6}_{-1.0}$	6.8	2.0	0.3	$5^{+19}_{-5} \pm 6$	52
ωK^{*0}	$7.0^{+5.2}_{-3.9}$	14	8.3	2.3	$9.1^{+6.7}_{-5.1} \pm 1.9$	19
$\rho^0\pi^+$	$26.1^{+9.1}_{-8.0}$	30	30	5.2	$15^{+5}_{-5} \pm 4$	
$\rho^-\pi^+$	$28.5^{+8.9}_{-7.9}$	12	12	5.6	$35^{+11}_{-10} \pm 5$	
$\rho^0\pi^0$	$3.4^{+5.2}_{-3.4}$	34	34			5.1
$\rho^0 K^+$	$14.8^{+8.8}_{-7.7}$	28	28			22
$\rho^- K^+$	$8.3^{+6.3}_{-5.0}$	11	11			25
$\rho^0 K^0$	$8.2^{+4.9}_{-3.9}$		10	2.7		27
$K^{*0}\pi^+$	$12.3^{+5.7}_{-4.7}$		18			27
$K^{*0}\pi^0$	$0.1^{+2.8}_{-0.1}$	37	24			4.2
$K^{*0}_{K^+\pi^-} K^+$	$0.0^{+2.1}_{-0.0}$		18			12
$K^{*+}_{K^0\pi^+} \pi^-$	$10.8^{+4.3}_{-3.5}$		7	5.2	$23^{+9}_{-7} \pm 3$	
$K^{*+}_{K^+\pi^0} \pi^-$	$5.7^{+4.3}_{-3.2}$		4.1	2.5	$20^{+15}_{-11} \pm 3$	
$K^{*+}\pi^-$				5.9	$22^{+8}_{-6} \pm 4$	
$K^{*+}_{K^0\pi^+} K^-$	$0.0^{+0.9}_{-0.0}$		7	0.0		8
$K^{*+}_{K^+\pi^0} K^-$	$0.0^{+1.3}_{-0.0}$		4.1	0.0		17
$K^{*+} K^-$				0.0		6
$\phi\pi^+$		54	27	0.0		4.0
$\phi\pi^0$		35	17	0.0		5.4
ϕK^+	$2.4^{+3.0}_{-1.9}$	53	26	1.3	$1.6^{+1.9}_{-1.2} \pm 0.2$	5.9
ϕK^0	$4.3^{+3.2}_{-2.3}$	41	7.0	2.6	$10.7^{+7.8}_{-5.7} \pm 1.1$	28

TABLE II. Final results and expectations from theoretical models.

Decay mode	$\mathcal{B}(10^{-6})$	Source	Theory \mathcal{B} (10^{-6})	References
$B^+ \rightarrow \omega\pi^+$	$11.3_{-2.9}^{+3.3} \pm 1.5$	This work	0.6 – 11	[3,5,9,10,26–29]
$B^0 \rightarrow \omega\pi^0$	< 5.8	This work	0.01 – 12	[3,5,10,26–29]
$B^+ \rightarrow \omega K^+$	< 8.0	This work	0.2 – 13	[3,5,9,10,26–29]
$B^0 \rightarrow \omega K^0$	< 21	This work	0.02 – 10	[3,5,10,26–29]
$B^+ \rightarrow \omega h^+$	$14.3_{-3.2}^{+3.6} \pm 2.1$	This work		
$B^+ \rightarrow \omega\rho^+$	< 47	This work	7 – 28	[3,5,8,27–29]
$B^0 \rightarrow \omega\rho^0$	< 11	This work	0.005 – 0.4	[3,27–29]
$B^+ \rightarrow \omega K^{*+}$	< 52	This work	0.9 – 15	[3,5,8,27–29]
$B^0 \rightarrow \omega K^{*0}$	< 19	This work	0.3 – 12	[3,5,27–29]
$B^+ \rightarrow \rho^0\pi^+$	$15_{-5}^{+5} \pm 4$	[20]	0.4 – 8	[3,11,5,9,10,26–29]
$B^0 \rightarrow \rho^-\pi^+$	$35_{-10}^{+11} \pm 5$	[20]	26 – 52	[3,11,5,10,26–29]
$B^0 \rightarrow \rho^0\pi^0$	< 5.1	This work	0.9 – 2.3	[3,11,10,26–29]
$B^+ \rightarrow \rho^0 K^+$	< 22	[20]	0.1 – 1.7	[2,3,5,9,10,26–29]
$B^0 \rightarrow \rho^- K^+$	< 25	[20]	0.2 – 2.5	[2,3,5,10,26–29]
$B^0 \rightarrow \rho^0 K^0$	< 27	[20]	0.04 – 1.7	[2,3,5,10,26–29]
$B^+ \rightarrow K^{*0}\pi^+$	< 27	[20]	4 – 12	[2,3,6,10,26–29]
$B^0 \rightarrow K^{*+}\pi^-$	$22_{-6}^{+8} \pm 4$	[20]	1.2 – 19	[2,3,5,10,26–29]
$B^0 \rightarrow K^{*0}\pi^0$	< 4.2	This work	1.1 – 5	[2,3,5,10,26–29]
$B^0 \rightarrow K^{*+}K^-$	< 6	[20]		
$B^+ \rightarrow K^{*0}K^+$	< 12	[20]	0.2 – 1	[3,9,10,26,28,29]
$B^+ \rightarrow \phi\pi^+$	< 4.0	[20]	0.001 – 0.4	[4–6,9,10,26–29]
$B^0 \rightarrow \phi\pi^0$	< 5.4	[20]	0.0004 – 0.2	[4–6,10,26–29]
$B^+ \rightarrow \phi K^+$	< 5.9	[20]	0.3 – 18	[2,3,5–7,9,10,26–29]
$B^0 \rightarrow \phi K^0$	< 28	[20]	0.3 – 18	[2,3,5–7,10,26–29]

distribution of \mathcal{H} is not known for these vector-vector final states we assume the worst case (\mathcal{H}^2) when computing the efficiency, and we require $\mathcal{H} < 0$ to reduce the large combinatoric background from soft π^0 's. This also results in much reduced cross-feed between the two decay modes.

As can be seen in Table I, we observe a clear signal for the decay $B^+ \rightarrow \omega\pi^+$. Figure 1 shows the contours in 1σ intervals of the likelihood function. Figures 2 and 3 show projections of the data on fit variables after tight selection cuts were applied on the variables other than the one plotted. The solid curves are not a fit to the data showed in each plot, but rather an overlay of the fit function scaled to take into account the additional cuts applied.

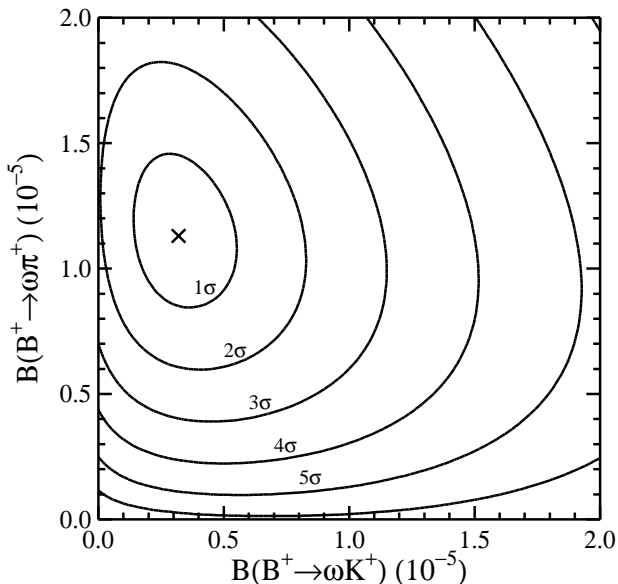


FIG. 1. Likelihood function contours for $B^+ \rightarrow \omega\pi^+$ and $B^+ \rightarrow \omega K^+$. Systematic errors are not included in the contours.

B. The decays $B^0 \rightarrow \rho^0\pi^0$ and $B^0 \rightarrow K^{*0}\pi^0$.

The results for the decay modes $B^0 \rightarrow \rho^0\pi^0$ and $B^0 \rightarrow K^{*0}\pi^0$ are based on a sample of $8.3 \times 10^6 B\bar{B}$ pairs. There is significant cross-feed between the two decay modes, due in large part to the presence of a high momentum π^0 in the final state, which results in poorer ΔE resolution. As a first step both decay modes are fit simultaneously. In this case, event selection prior to the maximum likelihood fit requires the invariant mass of the resonance to be within $0.3 < M_{h+h^-} < 1.0 \text{ GeV}/c^2$, as well as $-0.3 < \Delta E < 0.2 \text{ GeV}$. Both quantities are computed assuming that the two charged tracks are pions. The continuum background hypothesis in the ML fit is separated into four components, depending on the identity of the charged tracks (π^+ or K^+). For input to the ML fit, ΔE , the resonance mass, and \mathcal{H} are calculated assuming the two charged tracks are pions for the $\rho^0\pi^0$ signal and continuum background hypotheses, and assuming one charged track to be a kaon and the other a pion for the $K^{*0}\pi^0$ hypothesis. We also use the dE/dx information for the two charged tracks.

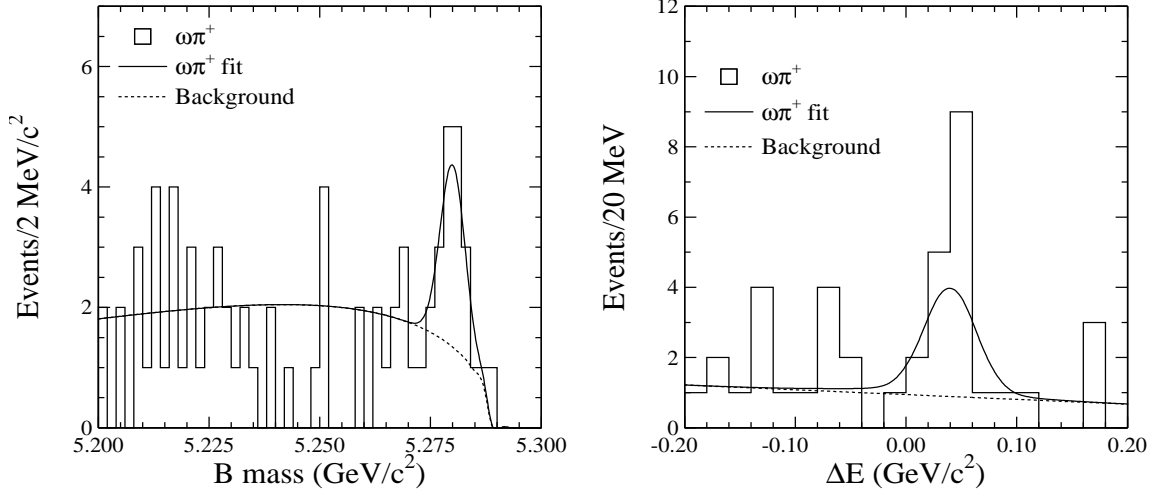


FIG. 2. Projection onto the reconstructed B mass (left) and ΔE (right) for $B^+ \rightarrow \omega\pi^+$. The solid line shows the result of the likelihood fit, scaled to take into account the cuts applied to variables not shown. The dashed line shows the background component.

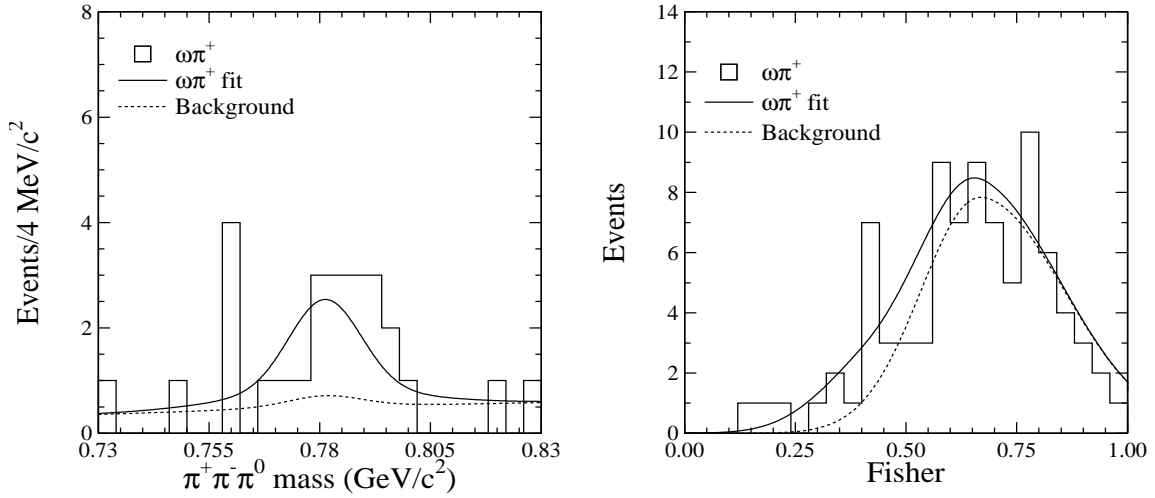


FIG. 3. Projection onto the reconstructed ω mass (left) and \mathcal{F} (right) for $B^+ \rightarrow \omega\pi^+$. The solid line shows the result of the likelihood fit, scaled to take into account the cuts applied to variables not shown. The dashed line shows the background component.

The results of this combined fit established that there is no significant signal for the decay mode $B^0 \rightarrow \rho^0\pi^0$. For this mode, the combined fit results are reported in Tables I and II.

A second ML fit was then performed for $B^0 \rightarrow K^{*0}\pi^0$ only. The preliminary selection required the dE/dx information for both the charged pion and charged kaon candidates in the final state to be within 2σ of the expected value. We also required $|\Delta E| < 0.2$ GeV, and that the resonance mass be within 150 MeV/ c^2 of the known K^{*0} mass. The ML fit looked for only two hypotheses, signal $K^{*0}\pi^0$ and continuum background. In this fit, no dE/dx information was used as input. No significant yield was observed, as indicated in Table I.

V. DISCUSSION

The observation of the decay $B^+ \rightarrow \omega\pi^+$ yields a branching fraction in complete agreement with the previously reported measurement for $B^+ \rightarrow \rho^0\pi^+$. For the corresponding neutral decay modes $B^0 \rightarrow \omega\pi^0$ and $B^0 \rightarrow \rho^0\pi^0$, fairly stringent upper limits are set, as could be expected because of their color suppression relative to the charged decay modes. For the latter decay mode, the upper limit from this work is another piece of information for studies of decays of the type $B \rightarrow \rho\pi$, to go along with the previous observations of $B^+ \rightarrow \rho^0\pi^+$ and $B^0 \rightarrow \rho^-\pi^+$ [20].

We also see evidence for the decay mode $B^0 \rightarrow \omega K^0$. In this case the charged decay mode $B^+ \rightarrow \omega K^+$ is expected to have a similar branching fraction. For this latter mode, the additional data and re-analysis of old data did not support the previously reported observation [19]. However, the central value for $B^+ \rightarrow \omega K^+$ is only about 1.5σ away from the central value for $B^0 \rightarrow \omega K^0$. There is no significant evidence for decays of the type $B \rightarrow \rho K$, although the results are consistent with the ones for $B \rightarrow \omega K$ decays.

The analysis presented here finds no significant yield for the decay mode $B^0 \rightarrow K^{*0}\pi^0$, in agreement with theoretical expectations which point to a branching fraction smaller than the previously observed $B^0 \rightarrow K^{*+}\pi^-$ [20]. There is no evidence for decay modes of the type $B \rightarrow K^*K$, as well as for ϕK and $\phi\pi$ final states.

VI. CONCLUSIONS

We have observed the decay mode $B^+ \rightarrow \omega\pi^+$, and measure a preliminary branching fraction of $\mathcal{B}(B^+ \rightarrow \omega\pi^+) = (11.3_{-2.9}^{+3.3} \pm 1.5) \times 10^{-6}$, in agreement with the previously reported observation of $B^+ \rightarrow \rho^0\pi^+$. We also see evidence for the decay $B^0 \rightarrow \omega K^0$. New upper limits are set for other final states including an ω meson, and for the decays $B^0 \rightarrow \rho^0\pi^0$ and $B^0 \rightarrow K^{*0}\pi^0$. In combination with previously reported measurements and upper limits, these results are generally in agreement with predictions based on factorization models in charmless hadronic B decays.

We gratefully acknowledge the effort of the CESR staff in providing us with excellent luminosity and running conditions. J.R. Patterson and I.P.J. Shipsey thank the NYI program of the NSF, M. Selen thanks the PFF program of the NSF, M. Selen and H. Yamamoto thank the OJI program of DOE, J.R. Patterson, K. Honscheid, M. Selen and V. Sharma thank the A.P. Sloan Foundation, M. Selen and V. Sharma thank the Research Corporation, F. Blanc thanks the Swiss National Science Foundation, and H. Schwarthoff and E. von Toerne

thank the Alexander von Humboldt Stiftung for support. This work was supported by the National Science Foundation, the U.S. Department of Energy, and the Natural Sciences and Engineering Research Council of Canada.

REFERENCES

- [1] M Kobayashi and T. Maskawa, Prog. Theor. Phys. **49**, 652 (1973).
- [2] N.G. Deshpande and J. Trampetic, Phys. Rev. D **41**, 895 (1990).
- [3] L.-L. Chau *et al.*, Phys. Rev. D **43**, 2176 (1991).
- [4] D. Du and Z. Xing, Phys. Lett. B **312**, 199 (1993).
- [5] A. Deandrea, N. Di Bartolomeo, R. Gatto, G. Nardulli, Phys. Lett. B **318**, 549 (1993);
A. Deandrea, N. Di Bartolomeo, R. Gatto, F. Feruglio, G. Nardulli, Phys. Lett. B **320**,
170 (1994).
- [6] R. Fleischer, Z. Phys. C **58**, 483 (1993); R. Fleischer, Phys. Lett. **B332**, 419 (1994).
- [7] A.J. Davies, T. Hayashi, M. Matsuda, and M. Tanimoto, Phys. Rev. D **49**, 5882 (1994).
- [8] G. Kramer, W. F. Palmer, and H. Simma, Nucl. Phys. B **428** 429 (1994).
- [9] G. Kramer, W. F. Palmer, and H. Simma, Zeit. Phys. C **66** 429 (1995).
- [10] D. Du and L. Guo, Z. Phys. C **75**, 9 (1997).
- [11] D. Ebert, R.N. Faustov, and V.O. Galkin, Phys. Rev. D **56**, 312 (1997).
- [12] M. Neubert and J. Rosner, Phys. Lett. **B 441**, 403 (1998).
- [13] N.G. Deshpande *et al.*, Phys. Rev. Lett. **82**, 2240 (1999).
- [14] X.-G. He, W.-S. Hou, and K.-C. Yang, preprint hep-ph/9902256, June, 1999.
- [15] Charge conjugate modes are implied throughout this paper.
- [16] F. Parodi, P. Roudeau, and A. Stocchi, preprint hep-ex/9903063, March, 1999; S. Mele,
Phys. Rev. **D59**, 113011, 1999.
- [17] CLEO Collaboration, Y. Kubota *et al.*, Nucl. Instrum. Methods Phys. Res., Sec. A **320**,
66 (1992).
- [18] T. Hill, Vertex 97, Rio de Janeiro, Brazil (1997).
- [19] CLEO Collaboration, T. Bergfeld *et al.*, Phys. Rev. Lett. **81**, 272 (1998).
- [20] CLEO Collaboration, Y. Gao and F. Würthwein, preprint hep-ex/9904008, May, 1999.
- [21] S. L. Wu, Phys. Rep. C **107**, 59 (1984).
- [22] E. Farhi, Phys. Rev. Lett. **39**, 1587 (1977).
- [23] CLEO Collaboration, D.M. Asner *et al.*, Phys. Rev. D **53**, 1039 (1996).
- [24] G. Fox and S. Wolfram, Phys. Rev. Lett. **41**, 1581 (1978).
- [25] GEANT 3.15, R. Brun *et al.*, CERN DD/EE/84-1.
- [26] N.G. Deshpande, B. Dutta, and S. Oh, Phys. Rev. D **57**, 5723 (1998).
- [27] M. Ciuchini *et al.*, Nucl. Phys. B **512**, 3 (1998).
- [28] A. Ali, G. Kramer, C.-D. Lu, Phys. Rev. D **59**, 014005 (1999).
- [29] Y.-H. Chen, H.-Y. Cheng, B. Tseng, and K.-C. Yang, preprint hep-ph/9903453, March,
1999.

Events

